Harmonic measure for critical Potts clusters

D. A. Adams, Yen Ting Lin, and L. M. Sander*
Department of Physics, University of Michigan, Ann Arbor, Michigan 48109-1040, USA

R. M. Ziff*
Department of Chemical Engineering, University of Michigan, Ann Arbor, Michigan 49109-2136, USA
(Received 13 July 2009; published 28 September 2009)

We present a technique, which we call "etching," which we use to study the harmonic measure of Fortuin-Kasteleyn clusters in the Q-state Potts model for $Q=1-4$. The harmonic measure is the probability distribution of random walkers diffusing onto the perimeter of a cluster. We use etching to study regions of clusters which are extremely unlikely to be hit by random walkers, having hitting probabilities down to 10^{-4600}. We find good agreement between the theoretical predictions of Duplantier and our numerical results for the generalized dimension $D(q)$ including regions of small and negative q.

DOI: 10.1103/PhysRevE.80.031141 PACS number(s): 64.60.ah, 05.45.Df, 64.60.al, 61.43.Hv

I. INTRODUCTION

A. Potts model

The Q-state Potts model, a generalization of the Ising model to Q different spins, has been the subject of considerable interest [1]. Two important cases are $Q=1$ and $Q=2$, which correspond to percolation [2] and the Ising model, respectively. When a Potts system is prepared at its critical temperature, subsets of the clusters of like spins, the Fortuin-Kasteleyn (FK) clusters [3,4] (to be defined below), are self-similar fractals [5]. For $Q=1$ the FK clusters are the same as the usual percolation clusters. In this paper, we will study the harmonic measure of the hulls of these fractal clusters for $Q=1,2,3,4$.

The harmonic measure may be thought of as the distribution of the surface electric field on a charged conductor. Since the Laplace equation and the steady-state diffusion equation are identical in form, the harmonic measure is also equal to the distribution of probabilities of random walkers diffusing far from the cluster onto a given section of the hull. In this paper, we use a biased random-walk sampling technique to obtain the harmonic measure. We also review other methods for measuring small probabilities and give details of our algorithms.

The harmonic measure is of practical interest because of its relation to the anomalous frequency dependence of the impedance of rough electrodes [6] and because of its obvious connection to processes that involve absorption of diffusing particles such as catalysis [7]. It has a deep connection to the structure of diffusion-limited aggregates (DLA) [8], since the harmonic measure determines where each walker will land; that is, for DLA it is the growth probability. In the case of critical Potts clusters and DLA, the harmonic measure is multifractal [9]. Advances in conformal field theory and Schramm-Loewner evolution have brought about renewed interest in the harmonic measure. In particular, certain aspects of the harmonic measure for Potts clusters can be computed in the continuum limit using these methods [10–15].

Numerical investigation of the harmonic measure of percolation [16] and DLA [16–18] clusters is difficult because the measure has a huge dynamic range for systems of even moderate size. In Refs. [16–18] one of two methods were used: the first is the straightforward one of releasing a large number of random walkers far from the cluster and determining where they land. The second uses relaxation or equivalent algorithms to solve the Laplace equation. The random walker method can only measure probabilities down to about 10^{-10} and samples a very small part of the measure for clusters of reasonable size. Relaxationlike methods are computationally costly and limited to small clusters and give similar lower limits on the probabilities that can be measured.

For DLA it is possible to go to much smaller probabilities by using the method of iterated conformal maps [19–21]. However, this technique is only capable of treating moderate size clusters [22]. In an earlier publication we generalized the random walker method and gave a technique capable of obtaining probabilities down to 10^{-300} for any fractal. We applied it to FK clusters for percolation and the Ising model [23]. This paper describes a further development of those techniques.

B. Generalized dimensions

The harmonic measure, the distribution of probabilities that random walkers will hit a given site on the perimeter of a cluster, is very complicated and varies wildly for the cases we are studying; see Fig. 1. A popular and useful way to characterize it is in terms of the generalized dimension, $D(q)$, of the measure. We define these objects as follows: we cover the hull with boxes of length L. With each box we associate a probability, p_i, which is the sum of the measure over the sites within the box. We then define a function $Z_L(q)$, sometimes called the partition function:

$$Z_L(q) = \sum_i p_i^q, \tag{1}$$

where q is some power [24]. If the object in question is fractal, then the partition function will follow a power law in L:

*Also at Michigan Center for Theoretical Physics, University of Michigan, Ann Arbor, MI 48109-1040.

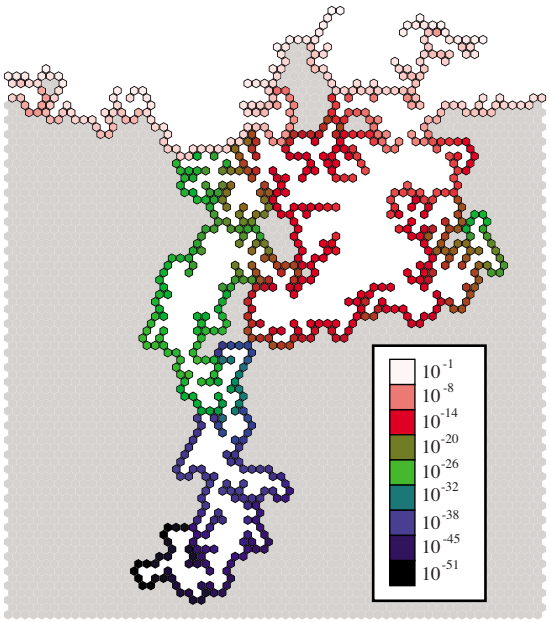

FIG. 1. (Color online) The harmonic measure for the complete perimeter of a small, $W=64$, percolation cluster. The solid gray regions represent the area that is inaccessible to the random walkers diffusing from above the cluster. Every perimeter site is colored according to its measure. The computation was performed using the etching method described below. Note that the measure on this small cluster spans 50 orders in magnitude.

$$Z_L(q) \sim (R/L)^{-\tau_q} = (R/L)^{-(q-1)D(q)} \tag{2}$$

for $(R/L) \to \infty$, where R is the size of the cluster. For integer q, $D(q)$ corresponds to the fractal dimension of the q-point correlation function. There are special values of $D(q)$. $D(0)$ is the fractal, box-counting, dimension of the hull. Also $D(1)$, the information dimension, is always unity by Makarov's theorem [25]. A related function is the singularity spectrum $f(\alpha)$, the Legendre transform of $D(q)$:

$$f(\alpha) = q\frac{d\tau}{dq} - \tau, \quad \alpha = \frac{d\tau}{dq}. \tag{3}$$

In this paper, we will focus exclusively on the $D(q)$. The singularity spectrum can be derived from our results using Eq. (3).

II. MODELS

A. Simulations of FK clusters for the Potts model

We produce critical Potts clusters in two ways. For percolation, we use the Leath algorithm [26]. The algorithm starts with a single active site; we attempt to turn its neighbors into active sites with probability p. If a conversion attempt fails, the site is labeled inactive. The process is repeated with neighbors of the active sites which have not been labeled as inactive. The process continues until there are no new active sites. If p equals p_c, the percolation threshold, a critical percolation cluster is produced. The outer layer of active sites is called the complete perimeter. Its fractal dimension is denoted D_H. The cluster of active sites is surrounded by a single layer of inactive sites; this layer is called the accessible (or exterior) perimeter [27] and has a fractal dimension denoted D_{EP}. The accessible perimeter of interest because, unlike the complete perimeter, it is expected to have a well-behaved limit when clusters are very large and are rescaled. The harmonic measure has been determined in this limit for the accessible perimeter of Potts clusters [10,11].

To obtain critical Potts clusters for $Q=2,3,4$, we grow equilibrated FK clusters using the Swendsen-Wang (SW) algorithm [28]. For any configuration of spins, FK clusters are subsets of clusters of like spins formed by a bond percolation process. That is, we consider the clusters formed when adjacent spins are connected with probability $p_c(Q)=1-\exp[-K_c(Q)]$, where $K_c(Q)$ is the critical coupling constant. For $Q=2,3,4$, on the triangular lattice, $p_c(Q)$ is known to be $1-1/\sqrt{3}$, $1-1/[1+\frac{1}{2}\sqrt{3}\sec(\pi/18)]$, and 1/2, respectively [29]. To obtain the equilibrium ensemble of FK clusters we iterate two steps until the system settles down (see below). The first step takes every current FK cluster and replaces the spin with one of the Q possible values, at random. In the second step, the bonds connecting the clusters are discarded and bond percolation is performed again, with $p=p_c(Q)$, on all neighboring sites with the same spin. The process is then repeated by updating the spins on the newly formed clusters. These two steps together constitute a spin update.

B. Parameters and observables

We grew critical Potts clusters for $Q=1-4$ on the triangular lattice, as described above. We chose to use a triangular lattice rather than a square lattice because the square lattice does not allow diffusion into fjords bounded by diagonal entrances. We use the width of the system, W, as the characteristic length. The clusters we want span in the width direction but not in the height direction. To make sure the clusters will only span in one direction, we chose very large aspect ratios. The height of the lattices were $100W$ and $8W$ for $Q=1$ and $Q>1$, respectively. We looked at six different system widths, $W=128,256,512,1024,2048,4096$. Because FK clusters are intrinsically bond clusters, we needed to use a trick to turn them into site clusters. We created a lattice twice as dense as the original and marked every site at the center of a bond and every site where two bonds meet as cluster sites. The FK cluster widths used were $W/2=64,128,256,512,1024,2048$.

To have proper FK clusters we require equilibration in the SW algorithm. We numerically determined that the equilibration time for $Q=2,3,4$ is of the order of W spin updates by looking at the relaxation of the average energy per spin and the average largest cluster size. For $Q=2,3$ and small W we ran a separate simulation to equilibrium for each spanning cluster which was added to our ensemble. For $Q=2$ and 3 and $W=2048$ and 4096 and for all of the $Q=4$ clusters, the equilibration time was too large to proceed in this way. In these cases we equilibrated the system once and recorded an ensemble of spanning clusters as the simulation proceeded. We conservatively estimate the correlation time as 50 spin updates for all W and Q. This means we recorded a spanning cluster every 50 spin updates.

For each system size we grew a number of clusters. For all Q our ensemble was 2000, 2000, 1000, 1000, 400, and 100 clusters for $W=128,256,512,1024,2048,4096$, respectively.

III. MEASURING SMALL PROBABILITIES WITH RANDOM WALKERS

A. Previous methods

Small probabilities in the harmonic measure correspond to very unlikely paths. As the simulation proceeds we can think of the event of a random walker landing where the measure is very small as a rare event. Thus, computing small probabilities is a similar task to finding the rate of a rare chemical reaction [30], a rare extinction of a disease [31] or a population [32], or the failure of a queuing system via queue overflow [33].

Accelerated numerical methods for these problems often involve biased event sampling. The sampling can frequently be cast as a random walk, either through state space or in our case, physical space. For example, one could ask what is the probability that a random walker starting halfway up a hill will successfully climb up to the top before sliding down to the bottom. If the hill is steep, it could be impossible to directly sample the probability to climb the hill. One could place barriers uniformly on the hill, which when crossed by the random walker, will split the random walker into two walkers, each with equal weight which add up to the original weight of the walker. This will aid sampling of the events higher up on the hill. This method is called "splitting" and effectively performs importance sampling [34]. One significant drawback of splitting is that if the barriers are too densely or sparsely spaced, the number of random walkers will tend to diverge or extinguish, respectively.

The methods we detail in this paper are related to the splitting method, but differ in that our methods do not have the possibility of diverging or extinguishing. Another popular method called "milestoning" [35] does not have a divergence problem, but does require the system studied to be in equilibrium and the location of the barrier to be known *a priori*, whereas our method works for equilibrium and nonequilibrium systems and the barriers are placed "on the fly."

B. Signposts

We have developed several accelerated methods for the harmonic measure problem. The motivation, as we have stated, is that it is usually impossible to send in enough random walkers to directly obtain the harmonic measure: the clusters will frequently have regions with probabilities of being hit that are smaller than 10^{-100}. It would require of order 10^{100} random walkers to sample this region; such a computation is clearly impossible.

We now review the first method we developed, the signpost method [23]. The signpost method consists of two steps which are applied iteratively; see Fig. 2. In the first (probe) step we release N diffusing random walkers far from the cluster to determine which regions are rarely visited in straightforward sampling. Next, we block off all poorly sampled regions with signposts (absorbing lines). In the second (measurement) step, N more walkers are released far from the cluster and either absorb on the cluster (or the accessible perimeter) or onto the signposts. The walkers sent in this step have their weight permanently added to the harmonic measure of the perimeter sites where they landed. In the next probe step, the walkers are released from the points on the signposts where the walkers in the previous measurement landed. The new walkers have a weight of p/N, where p is the fraction of random walkers that absorb onto signpost lines in the previous step, to conserve probability. The probe step again helps determine which regions are still poorly sampled, which are subsequently blocked off. Next, another measurement step is performed. This process is repeated until all regions are explored by the random walkers. This algorithm can be applied to on- and off-lattice clusters.

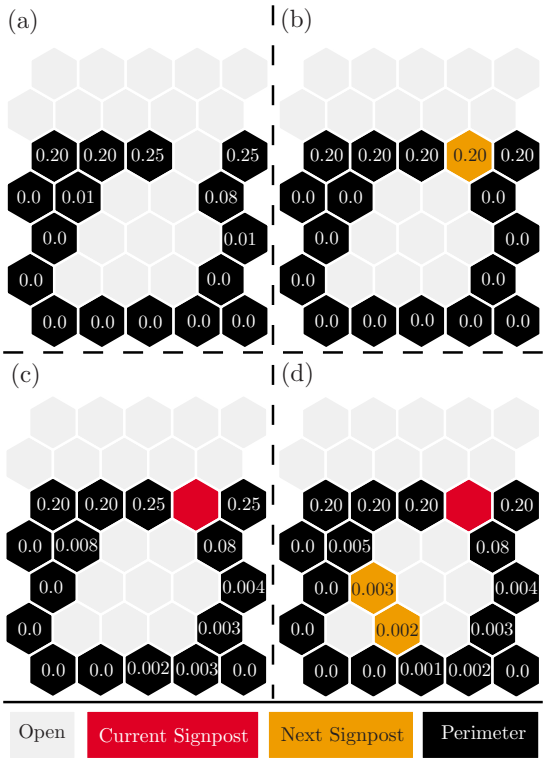

FIG. 2. (Color online) The signpost method. The system is periodic in the horizontal direction. (a) First (probe) step: N random walkers are released from the top row and absorb onto the perimeter sites. (b) We choose the first probability threshold as 0.1. Using this threshold, we connect the bounding sites using signpost sites. In the second (measurement) step we send N more random walkers from above which can absorb onto the signpost or perimeter sites. (c) Second probe step: the random walkers are launched from the signpost sites in the previous measurement step. The weights of the walkers released in this step have a weight of p/N where p is the fraction of the random walkers that hit the signpost site in (b). (d) The second threshold, 0.01, is used to determine the location of the new signpost sites.

We should note some things about this method. First, one must determine the entire perimeter of the cluster at the beginning of the computation in order to figure out how to block poorly sampled regions. Also, one needs to choose a

rate to reduce the threshold for calling areas "poorly sampled" in each iteration. In [23], we moved the threshold down by a power of 10 each iteration, whereas in [36], we reduced it as a function of how many walkers hit the signpost in the previous iteration. When more walkers hit the signposts we moved them even deeper. The second method gave more consistent walker saturation, which should lead to a slower compounding of error. It is important to note the signpost algorithm is only practical for two-dimensional problems. For higher dimensions, one would need to define signpost *surfaces* to block poorly sampled regions. This could be very complex for a complicated cluster.

C. Etching

We now describe the method we use here which we call "etching." Consider the hull of FK clusters grown on a triangular lattice with periodic boundary conditions. We want to find the harmonic measure of the top perimeter from above. To do this, we start by marking all sites that are exterior to the cluster from above as *soft* sites; the soft sites are absorbing like the cluster (or accessible perimeter) sites. The highest row is limited to one level above the highest point on the perimeter.

We next relabel every site on that highest row as a *current level* site; these are not absorbing. We release N random walkers, each with weight $1/(NW)$, from each current level site. The walkers released from these sites are allowed to walk until they deposit their weight onto a soft site or a perimeter site. If they move one level further away from the cluster, they are immediately moved back onto the current level sites using a Green's function which must be determined in advance. However, this is rather simple since it is the Green's function to return to a plane from one site above the plane. This Green's function is used for the entire simulation and limits how far a walker can backtrack to at most one level above the cluster. After all random walkers are released, the labels on each current level site are removed and every soft site hit in the previous step is labeled as a current level site. From each current level site i we release N random walkers with weight p_i, where p_i is the amount of probability deposited on the site in the previous step divided by N. This process is repeated until there are no more soft sites. See Fig. 3.

Etching can be thought of the limit of the signpost method with the signposts spaced one site apart. However, etching has several benefits over the signpost method. First, the entire perimeter of the cluster does not need to be mapped out before we start. Both algorithms have the same time complexity, $O(W^3)$ for the complete perimeter of Ising clusters, and both methods have similar memory requirements. In contrast to the signpost method, the etching method can be easily generalized to higher-dimensional lattice problems and networks. We have successfully used etching to obtain the harmonic measure of three-dimensional percolation clusters [37].

D. Green's functions

We have also developed a rare-event method which may be significantly more efficient than etching and signposting for some problems. Thus far we have applied this method only to simple test problems. This method manipulates probabilities directly and does not allow backtracking of probability. To do this, we calculate the Green's function $G(i,j;k,l)$, i.e., the probability to move to any of the sites i, j in the next level from a given site k, l in the current level.

To illustrate our algorithm, consider finding the probability distribution a channel with absorbing walls on a square lattice. The initial condition is that the probability is uniformly distributed among the sites in the first row of the channel and the zeroth row is a reflecting boundary. All sites that initially have probability are denoted by C. The previous level sites, absorbing sites, and next level sites accessible to the current level sites are denoted by B, A, and N, respectively. (Initially, the previous level is the reflecting boundary.) In each iteration, the goal is to move all of the probability from each current level site to all the next level and absorbing sites.

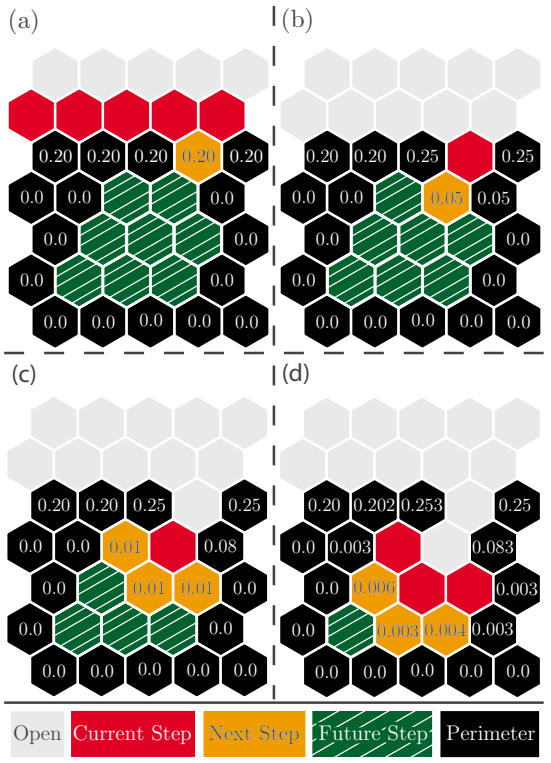

FIG. 3. (Color online) The etching method. Walkers are released from the current level sites. The next level of soft sites absorb walkers; they are then relabeled as current level sites. Future sites are all sites which will eventually become current level sites. The first round of random walkers is launched from the row above the cluster, (a). The weight of all of the walkers released is $0.2/N$, where N is the number of walkers released per current level site. 20% of the walker weight is deposited onto the top row of perimeter sites and the next level soft site, which will release N walkers in the next step. (b). One more perimeter site is accessible to the random walkers and 5% of the weight is deposited on the site in the next level. (c) Three sites in the next level each absorb 1% of the walker weight. (d) Due to the reduced weight of the walkers released in the next step, small probabilities are measured on the newly exposed perimeter sites.

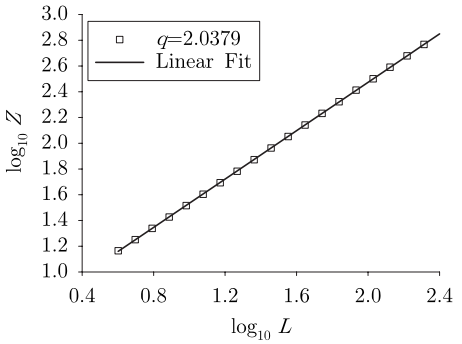

FIG. 4. An example of the fit of versus to a straight line for $q=2.0379$. The behavior is similar for all q values that we have examined. The slope of the line is $\tau(q) \equiv (q-1)D(q)$.

We find the Green's function by iteration on an index s. The process begins for some current level site, k, l; $(k,l) \in C$. Initially, probability only resides at k, l so that for $s=0$, $G^s(i,j;k,l)=\delta_{i,k}\delta_{j,l}$. In each iteration, the probability is moved to each of the current level site's neighbors,

$$G^{(s+1)}(i,j;k,l) = \sum_{(m,n)} W(i,j;m,n)G^{(s)}(m,n;k,l), \tag{4}$$

using the jump probability,

$$\begin{aligned} W(i,j;m,n) &= \frac{1}{4}(\delta_{i,m+1}\delta_{j,n} + \delta_{i,m-1}\delta_{j,n} + \delta_{i,m}\delta_{j,n+1} \\ &\quad + \delta_{i,m}\delta_{j,n-1}) \quad (m,n) \in C \\ &= G_B(i,j;m,n) \quad (m,n) \in B \\ &= \delta_{i,m}\delta_{j,n} \quad (m,n) \in A \cup N. \end{aligned} \tag{5}$$

Here $G_B(i,j;m,n)$ is the Green's function for the previous level, see below, and the last line represents the probability staying at absorbing and next level sites. $G_B(i,j;m,n)$ takes into account all the processes that would correspond to random walkers backtracking before the previous level. To start the process, the reflecting boundary has $G_B(i,j;0,n) = \delta_{i,1}\delta_{j,n}$.

For large s, virtually all of the probability will be on absorbing sites and next level sites. In any finite amount of time, some slight probability will remain in the current level, so after the stopping criterion is met, the probabilities recorded on the absorbing and next level sites must be normalized. When this has been achieved, we have the Green's function from a given site in the current level, k, l, to any site in the next level, i, j:

$$G_B(i,j;k,l) = \lim_{s\to\infty} G^{(s)}(i,j;k,l). \tag{6}$$

In the next step, this G_B will be used as a jump probability.

This process is repeated for all current level sites so that Green's functions from those sites to the next level sites and absorbing sites are calculated. With these Green's functions, it is easy to determine where the probability from the first level will end up. If the probability in the starting level is $P(k,l)$, then the probability in the next level is

$$P(i,j) = \sum_{(k,l)\in C} G_B(i,j;k,l)P(k,l). \tag{7}$$

Note that (i,j) can be absorbing sites as well as next level sites.

The next step is to relabel all current level sites as previous level sites, relabel all next level sites as current level sites, and mark all sites that are accessible to the new current level sites (which are not previous or absorbing sites) as next level sites. Then the process is repeated.

The end result of this process is that all of the original probability is at absorbing sites, as it would be using signposting or etching. Although this example contained only sites that were completely absorbing or nonabsorbing, the Green's function method can easily be generalized to partial absorption problems.

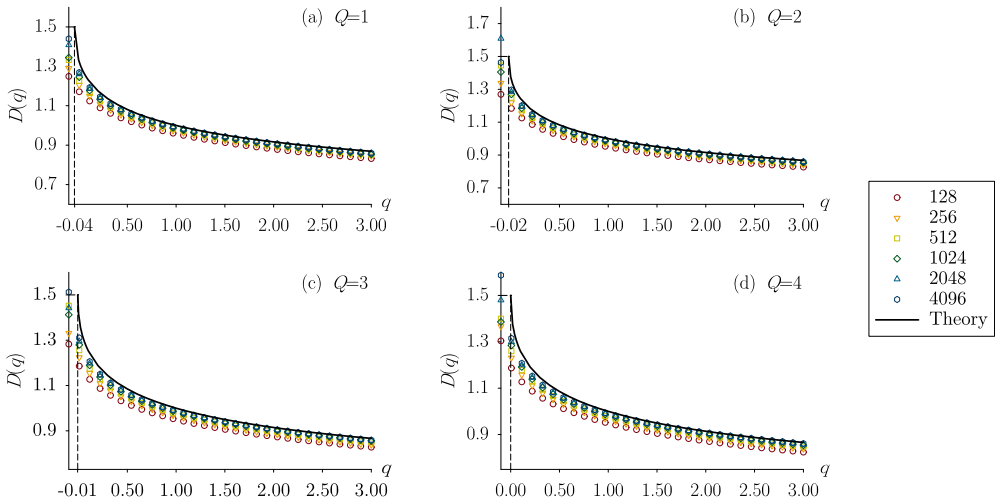

FIG. 5. (Color online) The $D(q)$ spectrum for the accessible perimeters of $Q=1,2,3,4$ clusters in (a), (b), (c), and (d), respectively. The solid lines are the theory of [11] and the symbols are the results of our simulations for several system widths. The vertical dotted lines mark q_{min} for the theoretical spectra for infinite systems.

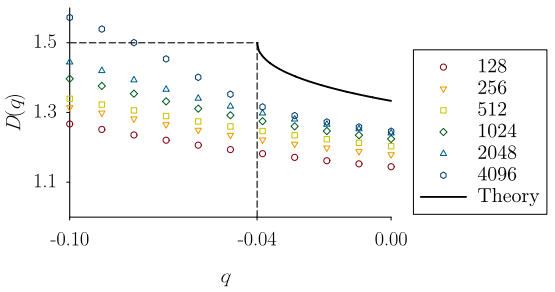

FIG. 6. (Color online) The $D(q)$ spectrum for the accessible perimeters of $Q=1$ clusters for small q. As the system size increases the simulated values increase, presumably to approach infinity for $q<-1/24$.

The Green's function method is somewhat more complex to program than the etching method and the simplest implementation involves setting up the Green's function lookups in sparse arrays. This leads to a memory complexity which grows like W^{2d}, where d is the dimension of the space. The memory complexity would significantly reduce its usefulness, as it would take at least 1 terabyte to store a two-dimensional cluster with a length scale of 1000 lattice sites. However, it is possible to store the Green's function lookup in an associative array; this reduces the memory complexity to W^{d-1+D}, where D is the fractal dimension of the perimeter. For the external perimeter of two-dimensional percolation clusters the memory complexity grows like $W^{7/3}$, which is quite close to the memory complexity for etching, W^2. For a cluster with a length scale of 1000 sites, the minimum required memory would be about 10 megabytes for the Green's function method.

IV. RESULTS

We used etching to find the harmonic measure of Q-state Potts model clusters. We analyze the measure by producing $D(q)$ spectra and histograms of the probability distributions. To obtain $D(q)$, we start by sectioning individual clusters into boxes of length L as described above. Because we are using a triangular lattice, it is convenient to use a parallelogram aligned with the lattice as a box. After completely tiling the cluster with boxes, we define the probability within a box $p_{i,L}$ as the sum of the measure of perimeter sites within the box. We then calculate $Z(L,q)$ using Eq. (1). $D(q)$ is related to $Z(L,q)$ by $(q-1)D(q)=m$, where m is the slope of $\log Z(L,q)$ versus $\log L$.

We found that for a given Q and q, all system sizes have similar local slope behavior over a range of L; see Fig. 4. In order to average over the ensemble we average $\log Z$. However, if we use the slopes for each individual member of the ensemble and average them we get virtually identical results.

The spectra of generalized dimensions for the external hulls of $Q=1-4$ are given in Fig. 5. In all cases the results are close to the theoretical predictions [11]. The theoretical predictions include a divergence of $D(q)$ for $q<q_{min}$ for an infinite system; see below. Our simulation results increase rapidly with W for this regime, as expected; see Fig. 6.

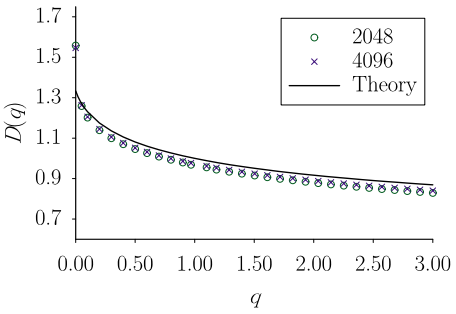

FIG. 7. (Color online) The $D(q)$ spectrum for $Q=1$ for the complete perimeter. There is no theoretical prediction for this quantity. However, for q substantially bigger than 0 we expect this result to be very similar to the result for the accessible perimeter since large probabilities will dominate the sum in Eq. (1). The line labeled "theory" is for the accessible perimeter.

For completeness, we include the spectrum of generalized dimensions for the complete perimeter for the case $Q=1$; see Fig. 7. There is no theoretical prediction for this quantity. For positive q the results are close to those of the accessible perimeter shown in Fig. 5. This is because, for positive q, large probabilities contribute most of the weight in $Z(q)$. Near $q=0$ the two spectra differ because there are significantly more sites with small measure for the complete hulls.

We also considered the distribution of the values of p directly, by making histograms of its frequency for all Q and W. The histograms turn out to be power laws with negative powers near -1; for an example see Fig. 8. Since the histogram is very accurately a power law in p, it is useful to plot the local slope of the histogram, which is shown in Fig. 9 for the accessible perimeters for $Q=1-4$. We also show the local slope for the complete perimeter of $Q=1$; see Fig. 10. The slope is calculated over about 10 orders of magnitude in p for the accessible perimeter, and more than one order of magnitude for the complete perimeter.

The significance of the slope is that it gives information about the nonscaling aspects of the distribution, and, in particular, the value of q_{min} mentioned above. If we call the slope of the histogram $-\phi$ (so that ϕ is a positive number) we see that the partition function of Eq. (1) formally diverges

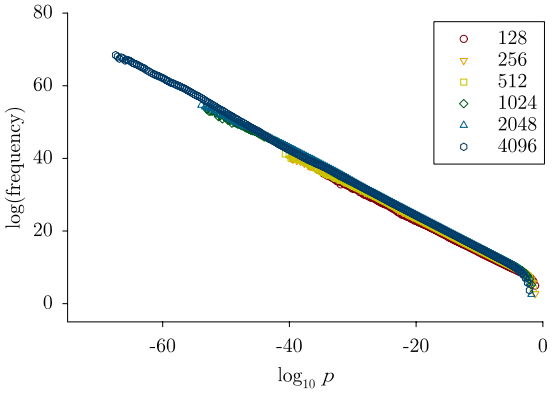

FIG. 8. (Color online) The histogram of the frequency of occurrence of the values of p for the accessible perimeter for $Q=1$. The points for various values of W are superimposed.

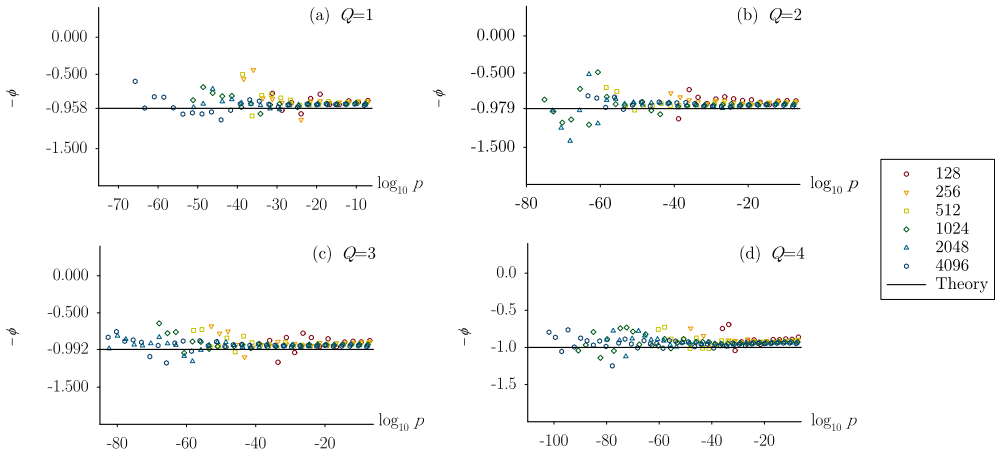

FIG. 9. (Color online) The local slope of the histogram of the frequency of occurrence of the values of p for the accessible perimeter for $Q=1,2,3,4$ in (a), (b), (c), and (d), respectively. Also shown (solid lines) are the theoretical predictions of the local slope from [11]. Note that in (b) the smallest probabilities recorded were not from the largest system size, but were from $W=1024$. This can be understood by the fact that ten times as many clusters were generated for $W=1024$. That is, among the many samples at $W=1024$, a few abnormally deep clusters were recorded which happened to have the smallest probabilities.

if $q<\phi-1$, or, said another way, we expect $D(q)$ to be undefined for $q<q_{min}=-1+\phi$. This means that the partition function is dominated by a few instances of very small probabilities which does not scale as power law in R/L. The values for the limit of the spectrum agree well with the predictions of Duplantier [10,11]; see Fig. 9. Note that the slopes are very nearly constant over about 40 orders of magnitude in p.

The slopes for the complete perimeter of percolation clusters are also constant over many orders of magnitude; see Fig. 10. In this case we find that ϕ is very close to 1 and the limit of the spectrum is at $q_{min}=0$. There is no theory for this case and no explanation for this intriguing result.

V. ERROR ESTIMATE

Since etching involves sampling the probability, there will be errors due to the finite number of random walkers released at each step. For the results in this paper, we released 10^3 random walkers per current level site for all system widths and Q values.

We can estimate the sampling errors as follows: we considered one percolation cluster with $W=2048$ and made ten independent computations of the p_i. The variance of the probability over this sample at a given point on the cluster, δp_i, is a measure of the reliability of the measurement. In our case we found that some points have a rather large percentage error, though always less than a factor of 3, but the average over all the points, $\langle \delta p_i/p_i \rangle$, was 23%. Note that the very small probabilities well inside the cluster have very small errors. There is no buildup of the error as we etch toward the interior, as might have been expected.

If it is necessary to reduce the error further, more random walkers can be used. However, we believe that the ensemble averaging that we did means that the generalized dimensions are much more accurate than the individual probabilities. Our evidence for the last statement is the good quality of the fit in Fig. 4 and the closeness of the results in Fig. 5 to theory. Note also that $D(0)$ is close to the known fractal dimensions of the exterior perimeters.

VI. CONCLUSIONS

In this paper, we presented the etching method, an accelerated technique for computing the harmonic measure. We are able to measure probabilities as small as 10^{-4600}. We showed how this method relates to other methods. We used etching to obtain the harmonic measure for the accessible perimeter of FK clusters for the Q-state Potts model for $Q=1-4$, for a range of system sizes. We compared this data to theoretical predictions [10,11]. These theories were produced for a continuum model which, in principle, might not apply to the scaling limit of the Q-state Potts model on a lattice. In fact, we found good agreement between our numerical results and the theoretical predictions for every comparison we made including the $D(q)$ spectra and the slopes of the power-law probability distributions.

For the complete perimeter of percolation clusters, we found the slope to be almost exactly -1 for about 4000 orders of magnitude. This suggests the smallest q for which

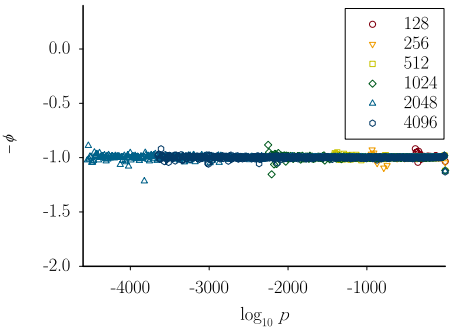

FIG. 10. (Color online) The local slope of the histogram of the frequency of occurrence of the values of p for the complete perimeter for $Q=1$.

$D(q)$ is defined is $q=0$. This means that there are many instances of small probabilities on the complete perimeter of percolation clusters which tend to diverge toward negative infinity faster than any power of R/L.

Etching, signposting, and the Green's function method are three tools which can find very small probabilities. The advantage of signposting is that it is natural to use in off-lattice systems, and, in fact, we have applied it to off-lattice DLA [36]. Etching is simple to program and should be easy to use in higher-dimensional on-lattice systems. Lastly, the Green's function method is likely to be the most efficient of the algorithms for on-lattice and network systems, but it is more difficult to implement and requires more memory than etching. The etching and Green's function methods (but not signposting) can be used in problems which involve absorption probabilities less than unity.

ACKNOWLEDGMENT

This work was supported in part by National Science Foundation Grant No. DMS-0553487.

[1] F. Y. Wu, Rev. Mod. Phys. **54**, 235 (1982).
[2] D. Stauffer and A. Aharony, *Introduction to Percolation Theory* (CRC Press, Boca Raton, 1994).
[3] C. M. Fortuin and P. W. Kasteleyn, Physica **57**, 536 (1972).
[4] P. W. Kasteleyn and C. M. Fortuin, J. Phys. Soc. Jpn. **S26**, 11 (1969).
[5] B. B. Mandelbrot, *The Fractal Geometry of Nature* (Freeman, San Francisco, 1982).
[6] T. C. Hasley and M. Leibig, Ann. Phys. **219**, 109 (1992).
[7] B. Sapoval, J. S. Andrade, and M. Filoche, Chem. Eng. Sci. **56**, 5011 (2001);M. Filoche, D. S. Grebenkov, J. S. Andrade, Jr., and B. Sapoval, Proc. Natl. Acad. Sci. **105**, 7636 (2008).
[8] T. A. Witten and L. M. Sander, Phys. Rev. Lett. **47**, 1400 (1981).
[9] B. B. Mandelbrot and C. J. G. Evertsz, Nature (London) **348**, 143 (1990).
[10] B. Duplantier, Phys. Rev. Lett. **82**, 3940 (1999).
[11] B. Duplantier, Phys. Rev. Lett. **84**, 1363 (2000).
[12] A. Belikov, I. A. Gruzberg, and I. Rushkin, J. Phys. A **41**, 285006 (2008).
[13] B. Duplantier and I. A. Binder, Nucl. Phys. B **802**, 494 (2008).
[14] E. Bettelheim, I. Rushkin, I. A. Gruzberg, and P. Wiegmann, Phys. Rev. Lett. **95**, 170602 (2005).
[15] I. A. Gruzberg, J. Phys. A **39**, 12601 (2006).
[16] P. Meakin, A. Coniglio, H. E. Stanley, and T. A. Witten, Phys. Rev. A **34**, 3325 (1986).
[17] R. C. Ball and O. R. Spivack, J. Phys. A **23**, 5295 (1990).
[18] W. G. Hanan and D. M. Heffernan, Phys. Rev. E **77**, 011405 (2008).
[19] M. B. Hastings and L. S. Levitov, Physica D **116**, 224 (1998).
[20] B. Davidovitch, A. Levermann, and I. Procaccia, Phys. Rev. E **62**, R5919 (2000).
[21] B. Davidovitch, M. H. Jensen, A. Levermann, J. Mathiesen, and I. Procaccia, Phys. Rev. Lett. **87**, 164101 (2001).
[22] M. H. Jensen, A. Levermann, J. Mathiesen, and I. Procaccia, Phys. Rev. E **65**, 046109 (2002).
[23] D. A. Adams, L. M. Sander, and R. M. Ziff, Phys. Rev. Lett. **101**, 144102 (2008).
[24] T. C. Halsey, M. H. Jensen, L. P. Kadanoff, I. Procaccia, and B. I. Shraiman, Phys. Rev. A **33**, 1141 (1986).
[25] N. Makarov, Proc. London Math. Soc. **51**, 369 (1985).
[26] P. L. Leath, Phys. Rev. B **14**, 5046 (1976).
[27] T. Grossman and A. Aharony, J. Phys. A **20**, 1193 (1987).
[28] R. H. Swendsen and J. S. Wang, Phys. Rev. Lett. **58**, 86 (1987).
[29] D. Kim and R. Joseph, J. Phys. C **7**, L167 (1974).
[30] N. G. van Kampen, *Stochastic Processes in Physics and Chemistry* (North-Holland, Amsterdam, 2001).
[31] H. Andersson and T. Britton, *Stochastic Epidemic Models and Their Statistical Analysis* (Springer, New York, 2000).
[32] M. S. Bartlett, *Stochastic Population Models in Ecology and Epidemiology* (Wiley, New York, 1961).
[33] J. Medhi and J. Medhi, *Stochastic Models in Queuing Theory* (Academic Press, Boston, 2003).
[34] J. M. Hammersley and D. C. Handscomb, *Monte Carlo Methods* (Methuen, London, 1965).
[35] A. K. Faradjian and R. Elber, J. Chem. Phys. **120**, 10880 (2004).
[36] D. A. Adams, L. M. Sander, E. Somfai, and R. M. Ziff, Europhys. Lett. **3**, 20001 (2009).
[37] D. A. Adams, L. M. Sander, and R. M. Ziff (unpublished).